Leg Kinematic Parameter Identification of Quadruped Robots Based on a Virtual Fixed Base

1st Chenxiang Yuan
School of Automation Science and Engineering,
Xi'an Jiaotong University,
Xi'an, China
19840937166@163.com

2nd Zhigang Ren*
School of Automation Science and Engineering,
Xi'an Jiaotong University,
Xi'an, China
renzg@xjtu.edu.cn

3rd Hui Chen
School of Automation Science and Engineering,
Xi'an Jiaotong University,
Xi'an, China
ch1102256774@163.com

Abstract: **The leg kinematic parameters of quadruped robots, including connecting rod length and joint angle, often deviate significantly due to machining and assembly errors. This inaccurate knowledge can lead to foot-end position errors and ultimately affect precise state estimation and control. Directing against this issue, this paper introduces the concept of a virtual fixed base and designs a non-redundant parameter identification method. The virtual fixed base is established by 4 marking points on the body, determining a hypothetical coordinate system, which is used to solve the hand-eye calibration problem of quadruped robots. This study provides the overall process of the kinematic parameter identification method. Simulation and experiment results show that the identified kinematic parameters converge to their actual value and the foot-end position accuracy is improved by over 80% after parameter compensation.**

Key-words: Kinematic parameter identification; Quadruped robots; Virtual fixed base; Hand-eye calibration; Least square method

I. Introduction

In recent years, the theoretical research and practical application of quadruped robots have made great progress[1-3]. However, the actual kinematic parameters of robots, including connecting rod length and joint angle, often deviate from the design values affected by factors such as machining accuracy and assembly errors. This will affect the accuracy of the kinematic model, leading to significant errors in foot-end position and velocity, ultimately affecting the control accuracy[4].

Compared with fixed-base heavy-duty industrial robots, there are few feasible methods to identify the kinematic parameters for quadruped robots. Most of the existing researches focuses on fixed-base heavy-duty industrial robots[5-8], which are not applicable for quadruped robots with a floating base. Zhu[9] proposed an effective kinematic self-calibration method for dual-manipulators based on virtual constraints to estimate the actual kinematic parameters of the robots. Du[10] designed an online robot calibration method that can quickly identify robotic kinematic parameters without stopping the robot, thereby greatly improving the operating efficiency of the robot. Zhang[11] presented an analytical method to determine the identifiable kinematic parameters for serial-robot calibration under various identification conditions.

Hand-eye calibration strategy is a key component in parameter identification[12-14]. Jiang[15] proposed a hand-eye calibration method based on the RGB-D camera reprojection error. Zhong[16] designed an adaptive controller to compute the orientation and position of the eye to the hand through a two-stage process, which enables parameter estimation in low-dimensional space. Jiang[17] significantly improved the localization accuracy of the robot by discussing a kinematic calibration method based on Extended Kalman Filtering and Particle Filtering. The traditional calibration method requires a fixed base coordinate system. However, the body of quadruped robots is usually considered as a floating base, which leads to uncertainty in the hand-eye transformation matrix. This means traditional hand-eye calibration strategies are not suitable for quadruped robots.

Directing against the above issues, this study introduces the concept of a virtual fixed base and designs a non-redundant parameter identification method based on the virtual fixed base. The leg of quadruped robots is similar to a serial robotic arm attached to the body. Therefore, the virtual fixed base is transformed from the floating base of a quadruped robot by fixing its body pose to set up a hypothetical coordinate system. The error parameter set is defined by combining non-redundant kinematic parameters with a high impact on the foot-end position [18-21], along with uncertain parameters of the hand-eye calibration matrix. A parameter error model and a least square identification method are established based on the DH parameter method.

The structure of this paper is as follows. Section II defines the coordinate system and establishes the single-legged kinematic model. Section III designs the overall scheme of parameter identification. Section IV involves simulations and experiments. Section V is the conclusion of this paper.

II. Kinematic Model

In this section, the 12-DOF series-legged quadruped robot is studied. To effectively analyze the kinematics of the quadruped robot, the relevant coordinate systems are defined and the single-legged kinematic model is established, which is the foundation of the identification method.

A. Coordinate System Definition

Based on the geometric structure of the 12-DOF series-legged quadruped robots, coordinate systems are established at the geometric center of the body, hip joint, and foot end, as shown in Fig.1. The specific definitions are as follows.

2024 9th International Conference on Automation, Control and Robotics Engineering (CACRE) | 979-8-3503-5030-2/24/$31.00 ©2024 IEEE | DOI: 10.1109/CACRE62362.2024.10635029

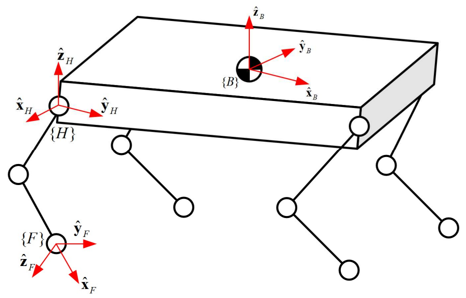

Fig. 1. Coordinate System Definition of Quadrupeds

$\{B\}$: Body coordinate system. The origin is located in the geometric center of the body, with the X-axis pointing directly in front of the body and the Z-axis pointing in the vertical body upward direction.

$\{H\}$: Hip joint base coordinate system. The origin is located in the center of the side-swinging hip joint, and the axis directions are fixed relative to the body.

$\{F\}$: Foot coordinate system. The origin is located in the center of the foot, and the axis directions are fixed relative to the foot.

B. Single-legged Kinematic Model

The single leg of a quadruped robot can be regarded as a serial robotic arm with 3 joints. Using the DH parameter method, it is easy to obtain ${}^{H}\mathbf{P}_F$, which is the foot-end position relative to the joint angle position described in the hip joint base coordinate system $\{H\}$. The kinematic model of a single leg can be obtained as follows:

$$ {}^{H}\mathbf{p}_F = \begin{bmatrix} c_1c_{23}l_2 + c_1c_2l_1 + s_1\omega \\ s_{23}l_2 + s_2l_1 \\ -s_1c_{23}l_2 - c_2l_1 + c_1\omega \end{bmatrix} \quad (1) $$

Where ω represents hip dislocation; l_1 and l_2 represent the connecting rod length of thigh and calf respectively; c_{ij} and s_{ij} represent $\cos(\theta_1 + \theta_2)$ and $\sin(\theta_1 + \theta_2)$ respectively.

III. Parameter Identification Method

A. Parameter Identification Process

The parameter identification process is as follows:

(1) **Modelling:** Establish the single-leg kinematic model of the quadruped robot.

(2) **Measurement:** Obtain the time-synchronized foot-end position and joint angle data.

(3) **Identification:** Input the foot-end position errors to get the identification values.

(4) **Compensation:** Compensate the single-leg model with kinematic parameter errors.

The kinematic parameter identification process is shown in Fig. 2. In identification, the foot-end position's Jacobian matrix is utilized as the parameter error model, and the identification method employs the least square approach. In measurement, a hand-eye calibration strategy is designed to uniform the measured foot-end positions and the nominal values, which are described in different coordinate systems. These positions are obtained by using a position-measuring device and the joint angles of the robot respectively.

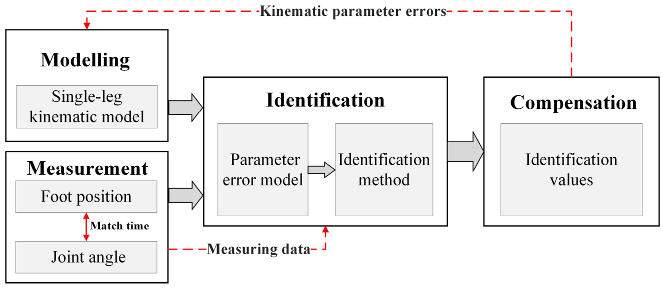

Fig. 2. Kinematic Parameter Identification Process

B. Hand-eye Calibration Strategy

The key to parameter identification is the hand-eye calibration. The measuring device acts as an "eye", capturing information about the foot-end position ${}^{S}\mathbf{p}_F^{rel}$ which is described in the measuring coordinate system $\{S\}$. The end of the robot acts as a "hand", and its nominal foot-end position ${}^{H}\mathbf{p}_F$ calculated by a kinematic model is described in $\{H\}$. To solve the inconsistency between "eye" and "hand" coordinate systems, it is essential to establish the transformation matrix from $\{H\}$ to $\{S\}$ ${}^{S}_{H}\mathbf{T}$ to unify the positional descriptions.

However, as shown in Fig. 3, since the coordinate system $\{B\}$ is attached to a floating base, the transformation matrix ${}^{S}_{B}\mathbf{T}$ is variable and difficult to measure, which makes the matrix ${}^{S}_{H}\mathbf{T}$ hard to calculate.

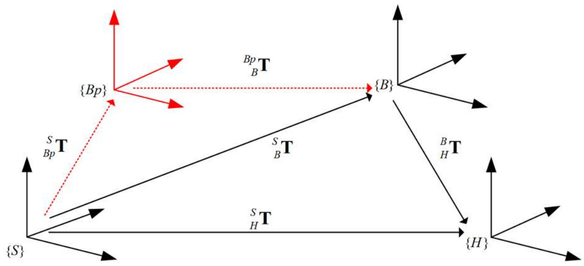

Fig. 3. Coordinate Transformation for Hand-eye Calibration

To solve the hand-eye calibration problem caused by the floating base, a parameter identification scenario applicable to quadruped robots is designed, as shown in Fig. 4.

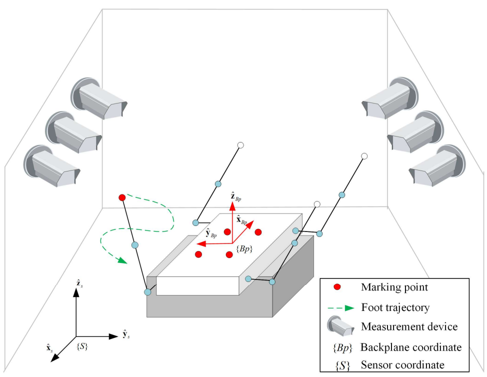

Fig. 4. Kinematics Parameter Identification Scenario

In Fig. 4, $\{S\}$ is the reference coordinate system of the measuring device. 4 points are marked at the body to conveniently introduce the backplane coordinate system $\{Bp\}$ as a virtual fixed base. The robot is fixed in a lying position on a platform and its legs move continuously to cover the maximum motion range. Meanwhile, an optical motion capture system works as the position-measuring device to obtain real-time foot-end positions by capturing the coordinates of marker points.

${}_{H}^{S}\mathbf{T}$ can be decomposed into 3 parts by introducing the $\{Bp\}$ coordinate system, as shown in Fig. 3.

$$ {}_{H}^{S}\mathbf{T} = {}_{Bp}^{S}\mathbf{T}\,{}_{B}^{Bp}\mathbf{T}\,{}_{H}^{B}\mathbf{T} \tag{2} $$

Where, ${}_{H}^{B}\mathbf{T}$ is determined by the body length l_b and width ω_b of the quadruped robot. And there are only translational and rotational relations in the Z-axis between the $\{Bp\}$ system and the $\{B\}$ system. The rotation angle is defined as α_h and the translational distance as z_h, which can be determined by measurement.

The expression of ${}_{B}^{Bp}\mathbf{T}$ is as follows:

$$ {}_{B}^{Bp}\mathbf{T} = \mathbf{R}_{\mathrm{Z}}(\alpha_{\mathrm{h}})\mathbf{D}_{\mathrm{Z}}(\mathrm{z_h}) = \begin{bmatrix} \cos(\alpha_{\mathrm{h}}) & -\sin(\alpha_{\mathrm{h}}) & 0 & 0 \\ \sin(\alpha_{\mathrm{h}}) & \cos(\alpha_{\mathrm{h}}) & 0 & 0 \\ 0 & 0 & 1 & \mathrm{z_h} \\ 0 & 0 & 0 & 1 \end{bmatrix} \tag{3} $$

Where, $\mathbf{R}_{\mathrm{Z}}(\alpha_{\mathrm{h}})$ is the rotation transformation matrix around the Z-axis. $\mathbf{D}_{\mathrm{Z}}(\mathrm{z_h})$ is the translation transformation matrix along the Z-axis.

Therefore, the key to the hand-eye calibration problem can be transformed into determining ${}_{Bp}^{S}\mathbf{T}$, which is to calculate ${}_{Bp}^{S}\mathbf{p}$ and ${}_{Bp}^{S}\mathbf{R}$. The specific steps are as follows:

1) Calculate ${}_{Bp}^{S}\boldsymbol{p}$

Assume the origin of $\{Bp\}$ as the center point of the 4 marked points, the expression is as follows:

$$ {}_{Bp}^{S}\mathbf{p} = \sum_{\mathrm{i}=1}^{4} \mathbf{p}_{\mathrm{i}} \tag{4} $$

2) Calculate ${}_{Bp}^{S}\boldsymbol{R}$

The rotation matrix can be composed of column vectors with unit axes.

$$ {}_{Bp}^{S}\mathbf{R} = [{}^{S}\hat{\mathbf{x}}_{Bp} \quad {}^{S}\hat{\mathbf{y}}_{Bp} \quad {}^{S}\hat{\mathbf{z}}_{Bp}] \tag{5} $$

By noting the positions of the marker points in Fig. 1 as $\mathbf{p}_1$、$\mathbf{p}_2$、$\mathbf{p}_3$、$\mathbf{p}_4$ in counter-clockwise order, starting from the left front, ${}^{S}\hat{\mathbf{x}}_{Bp}$ and ${}^{S}\hat{\mathbf{z}}_{Bp}$ can be represented by the coordinates of the 4 marker points.

${}^{S}\hat{\mathbf{x}}_{Bp}$ can be expressed as:

$$ {}^{S}\hat{\mathbf{x}}_{Bp} = \frac{\mathbf{p}_1 + \mathbf{p}_4 - \mathbf{p}_2 - \mathbf{p}_3}{\|\mathbf{p}_1 + \mathbf{p}_4 - \mathbf{p}_2 - \mathbf{p}_3\|_2} \tag{6} $$

${}^{S}\hat{\mathbf{z}}_{Bp}$ can be expressed as:

$$ {}^{S}\hat{\mathbf{z}}_{Bp} = \frac{(\mathbf{p}_1 - \mathbf{p}_2) \times (\mathbf{p}_3 - \mathbf{p}_4)}{\|(\mathbf{p}_1 - \mathbf{p}_2) \times (\mathbf{p}_3 - \mathbf{p}_4)\|_2} \tag{7} $$

Therefore, ${}^{S}\hat{\mathbf{y}}_{Bp}$ can be expressed as:

$$ {}^{S}\hat{\mathbf{y}}_{Bp} = \frac{{}^{S}\hat{\mathbf{z}}_{Bp} \times {}^{S}\hat{\mathbf{x}}_{Bp}}{\left\| {}^{S}\hat{\mathbf{z}}_{Bp} \times {}^{S}\hat{\mathbf{x}}_{Bp} \right\|_2} \tag{8} $$

After the Smithsonian orthogonalization of each unit axis, the final rotation matrix ${}_{Bp}^{S}\mathbf{R}$ is obtained.

C. Error Parameter Set

The single-legged kinematic model is established using DH parameters. For a 3-joint serial robotic arm, it is theoretically necessary to identify 16 linkage parameters in 4 groups. Some of these kinematic parameters have the same effect on the foot-end position, which means that there are redundant parameters in the identification model. Therefore, only 3 joint angle biases and 3 connecting rod lengths are selected as the parameters to be identified.

In addition, during hand-eye calibration, inaccurate positions of the marking points may lead to small deviations in ${}_{Bp}^{B}\mathbf{T}$. Therefore, α_h and z_h are also considered as parameters to be identified.

The error parameter set can be defined as follows:

$$ \Delta\Theta = [\Delta\theta_1\ \Delta\theta_2\ \Delta\theta_3\ \Delta\omega\ \Delta l_1\ \Delta l_2\ \Delta\alpha_{\mathrm{h}}\ \Delta z_{\mathrm{h}}]^{\mathrm{T}} \tag{9} $$

Based on the error parameter set, the parameter error model can be obtained.

D. Parameter Error Model

Taking $\{Bp\}$ as the fixed base coordinate system in the parameter identification process, the parameter error model is the mapping matrix of the position vector deviation $\Delta{}_{F}^{Bp}\mathbf{p}$ with respect to the error parameter $\Delta\Theta$. Based on the single-legged kinematics and the transferability of the transformation matrix, the expression ${}_{F}^{Bp}\mathbf{p}$ is as follows:

$$ {}_{F}^{Bp}\mathbf{p} = {}_{B}^{Bp}\mathbf{T}\,{}_{H}^{B}\mathbf{T}\,{}_{F}^{H}\mathbf{p} = $$

$$ \begin{bmatrix} c_{\alpha_h}(s_{23}l_2 + s_2l_1 + 0.5l_b) + s_{\alpha_h}(c_1c_{23}l_2 + c_1c_2l_1 + s_1\omega - 0.5\omega_b) \\ s_{\alpha_h}(s_{23}l_2 + s_2l_1 + 0.5l_b) - c_{\alpha_h}(c_1c_{23}l_2 + c_1c_2l_1 + s_1\omega - 0.5\omega_b) \\ -s_1c_{23}l_2 - s_1c_2l_1 + c_1\omega + z_h \end{bmatrix} \tag{10} $$

Assuming that the deviations are small enough, the expression of $\Delta{}_{F}^{Bp}\mathbf{p}$ can be obtained by taking the partial derivation of formula (10) with respect to Θ:

$$ \Delta{}_{F}^{Bp}\mathbf{p} = \mathbf{J}(\Theta)\Delta\Theta \tag{11} $$

The expression $\mathbf{J}(\Theta)$ is as follows:

$$ \mathbf{J}(\Theta) = \begin{bmatrix} -s_{\alpha_h}(s_1c_{23}l_2 + s_1c_2l_1 - c_1\omega) & c_{\alpha_h}(c_{23}l_2 + c_2l_1) - s_{\alpha_h}(c_1s_{23}l_2 + c_1s_2l_1) & c_{\alpha_h}c_{23}l_2 - s_{\alpha_h}c_1s_{23}l_2 & s_{\alpha_h}s_1 & c_{\alpha_h}s_2 + s_{\alpha_h}c_1c_2 & c_{\alpha_h}s_{23} + s_{\alpha_h}c_1c_{23} \\ c_{\alpha_h}(s_1c_{23}l_2 + s_1c_2l_1 - c_1\omega) & s_{\alpha_h}(c_{23}l_2 + c_2l_1) + c_{\alpha_h}(c_1s_{23}l_2 + c_1s_2l_1) & s_{\alpha_h}c_{23}l_2 + c_{\alpha_h}c_1s_{23}l_2 & -c_{\alpha_h}s_1 & s_{\alpha_h}s_2 - c_{\alpha_h}c_1c_2 & s_{\alpha_h}s_{23} - c_{\alpha_h}c_1c_{23} \\ -c_1c_{23}l_2 - c_1c_2l_1 - s_1\omega & s_1s_{23}l_2 + s_1s_2l_1 & s_1s_{23}l_2 & c_1 & -s_1c_2 & -s_1c_{23} \end{bmatrix} $$

$$
\begin{matrix} -s_{\alpha_h}(s_{23}l_2 + s_2 l_1 + 0.5l_b) + c_{\alpha_h}(c_1 c_{23} l_2 + c_1 c_2 l_1 + s_1\omega - 0.5\omega_b) & 0 \\ c_{\alpha_h}(s_{23}l_2 + s_2 l_1 + 0.5l_b) + s_{\alpha_h}(c_1 c_{23} l_2 + c_1 c_2 l_1 + s_1\omega - 0.5\omega_b) & 0 \\ 0 & 1 \end{matrix}\Bigg] \tag{12}
$$

E. Least Square Parameter Identification Method

The leg joints are controlled to move continuously to cover the maximum motion range. Then taking n sets of foot-end positions and joint angles, identification equations for the kinematic parameters can be obtained by using the least square method.

$$\Delta\widehat{\Theta} = (\hat{\mathbf{J}}(\Theta)^{\mathrm{T}}\hat{\mathbf{J}}(\Theta))^{-1}\hat{\mathbf{J}}(\Theta)^{\mathrm{T}}\Delta^{Bp}\widehat{\mathbf{p}}_F \tag{13}$$

Where,

$$\hat{\mathbf{J}}(\Theta) = [\mathbf{J}^{\mathrm{T}}(\Theta_1) \quad \mathbf{J}^{\mathrm{T}}(\Theta_2) \quad \ldots \quad \mathbf{J}^{\mathrm{T}}(\Theta_n)]^{\mathrm{T}} \tag{14}$$

$$\Delta^{Bp}\widehat{\mathbf{p}}_F = [\Delta^{Bp}\mathbf{p}_{F1}^{\mathrm{T}} \quad \Delta^{Bp}\mathbf{p}_{F2}^{\mathrm{T}} \quad \ldots \quad \Delta^{Bp}\mathbf{p}_{Fn}^{\mathrm{T}}]^{\mathrm{T}} \tag{15}$$

$$\Delta^{Bp}\mathbf{p}_{Fi} = {}^{Bp}\mathbf{p}_{Fi}^{\mathrm{r}} - {}^{Bp}\mathbf{p}_{Fi}^{\mathrm{n}} \tag{16}$$

In formula (16), ${}^{Bp}\mathbf{p}_{Fi}^{\mathrm{r}}$ is the actual foot-end position, which can be obtained by converting the coordinate system with ${}^{S}\mathbf{p}_{Fi}^{\mathrm{r}}$ captured by the measuring device. ${}^{Bp}\mathbf{p}_{Fi}^{\mathrm{n}}$ is the nominal foot-end position, which can be obtained by converting the coordinate system with ${}^{B}\mathbf{p}_{Fi}^{\mathrm{n}}$.

F. Algorithmic Pseudo-code

Based on the above parameter identification scheme, the pseudo-code of the algorithm is as follows.

Algorithm *Non-redundant Parameter Identification Method Based on A Virtual Fixed Base*

Input: n sets of joint angles $\boldsymbol{\theta}$, foot-end position ${}^{S}\mathbf{p}_F^{rel}$
Output: results of error parameter $\Delta\boldsymbol{\Theta}$
Initialization: body marker position coordinates, nominal kinematic model parameters
1: Obtain ${}_{Bp}^{S}\mathbf{T}$ based on formula (4~8)
2: Obtain ${}^{Bp}\mathbf{p}_{Fi}^{r}$ by transforming the coordinate of ${}^{S}\mathbf{p}_{Fi}$
3: Obtain ${}^{Bp}\mathbf{p}_{Fi}^{n}$ based on formula (10)
4: Obtain $\Delta_{F}^{Bp}\mathbf{p}$ based on formula (15) and (16)
5: Obtain $\hat{J}(\boldsymbol{\Theta})$ based on formula (12) and (14)
6: Obtain $\Delta\widehat{\boldsymbol{\Theta}}$ *based on formula (13)*
7: Return $\Delta\widehat{\boldsymbol{\Theta}}$

IV. Simulation And Experiment

A. Simulation analysis

1) Parameter setting and simulation process

Referring to the kinematic parameters of the A1 robot and taking the left front leg as an example, the nominal, actual, and error values of the kinematics are set before simulation, as shown in Table 1. Set the error ranges of the joint angle and measuring devices as [-1.0*deg*,1.0*deg*], [-1.0*mm*,1.0*mm*] respectively to simulate the noise of sensors. The simulation process is as follows:

Firstly, Use the nominal kinematic parameters Θ^n in Table 1 to build the pre-identification single-legged kinematic model and the parameter error model; Use the real kinematic parameters Θ^r to obtain the real kinematic model. Then, randomly select 1000 groups of target sampling points, and input the above data into the models. Jacobian matrix of the foot-end position error and the parameter error model can be obtained subsequently. Finally, use the least square method to obtain the identification results.

2) Result analysis

The kinematic parameters were identified using the data of 1000 target sampling points. The results are shown in Table 2. The average percentage error of the error parameters identification results was 91.87%. Taking the absolute accuracy of the foot-end position as the evaluation index, the root mean square error(RMSE) of the foot-end position was 16.5*mm* before identification, and it was reduced to 1.0*mm* after identification. The average accuracy was improved by 94.16%.

The above data illustrate the effectiveness of the algorithm. Fig. 5 shows the curve of the kinematic parameter identification results with respect to the number of target sampling points. It is evident that as the number of sampling points increases, the identification results for each parameter gradually approach the actual value, indicating rapid convergence.

Fig. 6 shows the visualization of the nominal and actual foot-end positions. Before compensation, the position error is obvious, and the error is reduced and close to the actual value after compensation.

TABLE I. Simulation Parameters of Kinematics Identification (Taking the Left Front Leg as AN Example)

Parameter	$\theta_1^{init}\backslash deg$	$\theta_2^{init}\backslash deg$	$\theta_3^{init}\backslash deg$	$\omega\backslash m$	$l_1\backslash m$	$l_2\backslash m$	$z_h\backslash m$	$\alpha_h\backslash deg$	$l_b\backslash m$	$\omega_b\backslash m$
Nominal value $\boldsymbol{\Theta}^n$	0.0	0.0	0.0	-0.08	0.2	0.2	0.06	0.0	0.361	0.094
Actual value $\boldsymbol{\Theta}^r$	1.0	1.5	2.0	-0.0838	0.21	0.22	0.065	3.0	0.361	0.094
Error value $\Delta\boldsymbol{\Theta}$	1.0	1.5	2.0	-0.0038	0.01	0.02	0.005	3.0	0.0	0.0

TABLE II. Simulation Results of Kinematics Identification (Taking the Left Front Leg as An Example)

Error parameter	$\Delta\theta_1$	$\Delta\theta_2$	$\Delta\theta_3$	$\Delta\omega$	Δl_1	Δl_2	Δz_h	$\Delta\alpha_h$
Identification value	1.200*deg*	1.536*deg*	2.275*deg*	-0.00348*m*	0.0098*m*	0.194*m*	0.0048*m*	3.112*deg*
Actual value	1.000*deg*	1.500*deg*	2.000*deg*	-0.00380*m*	0.0100*m*	0.020*m*	0.005*m*	3.000*deg*
Accuracy rate	77.8%	95.7%	86.4%	88.9%	97.7%	96.9%	96.3%	95.2%

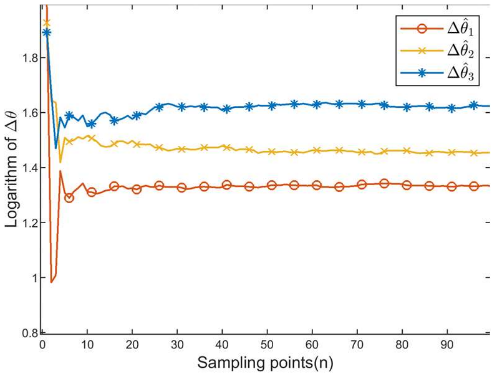

(a)Joint Angle Deviation

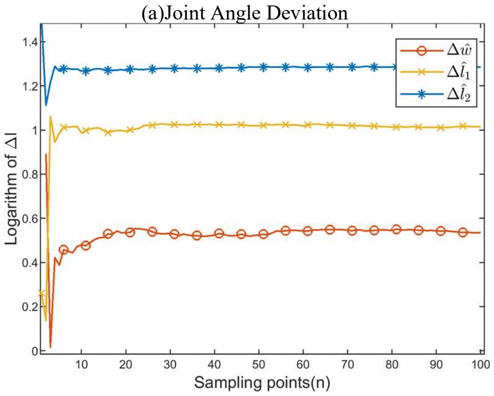

(b)Connecting Rod Deviation

Fig. 5. Kinematic Parameter Identification Results

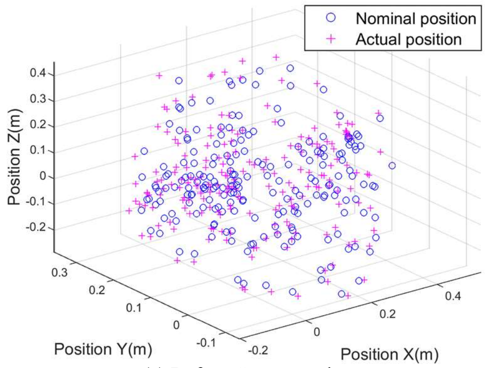

(a) Before Compensation

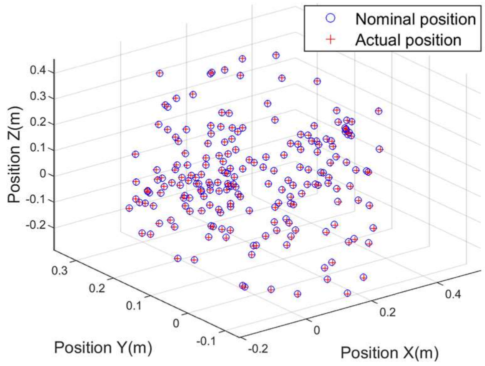

(b) After Compensation

Fig. 6. Comparison of Foot-end Position Error in Simulation

B. Experimental setting and analysis

1) Experimental setting

In order to verify the reliability of the method in this paper, the leg kinematic parameters of the actual robot are calibrated. The NOKOV optical motion capture system was used as the measuring device, which utilized optical imaging technology to capture the coordinates of the marked points in real time with sub-millisecond accuracy. The experimental scenario is shown in Fig. 7, where marker points are installed at the body and foot end of the A1 robot, and the joints of a single leg are sequentially controlled to move in a wide range of periodic motions. ROS nodes were used to capture the joint information of the A1 robot and point information of the measuring device during the motion process. After time synchronization on this information, the initial experimental data is obtained.

Fig. 7. Parameter Recognition Experimental Scenarios

2) Result analysis

Taking the left front leg as an example, the kinematic error parameters of the actual robot are identified as $\Delta\Theta_{FL} = [1.611deg, 0.178deg, 5.714deg, 2.22mm, 1.41mm, 16.1mm]$. The data show that all joint angles of the robot have some bias, and the calf rod length errors are comparatively large. Using the point information of the measuring device as reference data, the RMSE of the foot-end position after compensation is reduced from 22.2mm to 3.90mm, with an accuracy improvement of 82.43%. Fig. 8 shows the foot-end position error before and after parameter compensation, which shows that the compensated foot-end position is very close to the actual value, and the error is significantly reduced.

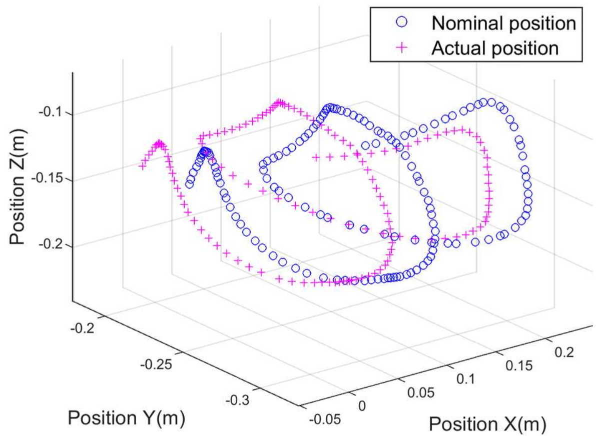

(a) Before Compensation

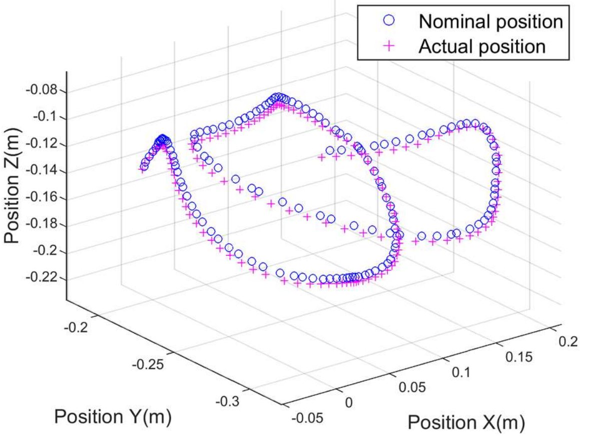

(b) After Compensation

Fig. 8. Comparison of Foot-end Position Error in Simulation

V. CONCLUSION

In this paper, a leg kinematic parameter identification method for quadruped robots based on a virtual fixed base is presented, which solves the problem of reduced control accuracy caused by inaccurate kinematic parameters. By fixing the pose of the body and introducing the virtual fixed base, a new hand-eye calibration strategy applicable to the quadruped robot is designed, and the corresponding kinematic parameter identification scheme is proposed. The simulation results show that the error parameters can rapidly converge to the accurate values, and the experimental results show that the position error of the foot end is significantly reduced after parameter compensation. This verifies the effectiveness and practicality of the method.

REFERENCES

[1] Liang Z X. “A review of motion control methods and bionic control theory for quadruped robots,” Proceedings 2022 IEEE Conference on Telecommunications, Optics and Computer Science (TOCS), Dalian, China, pp. 928-931.

[2] Li Y B, Li B, Ruan J H, and Rong X W, “Research of mammal bionic quadruped robots: A review,” Proceedings 2011 IEEE 5th International Conference on Robotics, Automation and Mechatronics (RAM), Qingdao, China, pp. 166-171.

[3] Wang C L, Li Y J, Sun H F, Hou X N, Fan C H and Yang Y, “The Dynamics Research of Quadruped Robotics with Flexible Spine: A Review,” Proceedings 2021 6th International Conference on Control, Robotics and Cybernetics (CRC), Shanghai, China, pp. 13-18.

[4] Yang S, H. Choset and Z. Manchester, “Online Kinematic Calibration for Legged Robots,” IEEE Robotics and Automation Letters, vol. 7, no. 3, pp. 8178-8185.

[5] Geng T, Geng J, Wang H T, Zhu B and Zhang C, “Calibration of Kinematic Parameters of Industrial Robot Based on Binocular Vision and Distance Error Model,” Proceedings 2023 5th International Conference on Artificial Intelligence and Computer Applications (ICAICA), Dalian, China, pp. 792-799.

[6] Zhao H H, Zhao J, Lin Y, Han Q F and Chen M P, “A New Calibration Method and Experimental Study for Kinematic Parameters of Industrial Robot,” Proceedings 2020 International Conference on Artificial Intelligence and Electromechanical Automation (AIEA), Tianjin, China, pp. 221-227.

[7] Xu X B et al., “A Novel Calibration Method for Robot Kinematic Parameters Based on Improved Manta Ray Foraging Optimization Algorithm,” IEEE Transactions on Instrumentation and Measurement, vol. 72, pp. 1-11.

[8] I. -W. Park, B. -J. Lee, S. -H. Cho, Y. -D. Hong and J. -H. Kim, “Laser-Based Kinematic Calibration of Robot Manipulator Using Differential Kinematics,” IEEE/ASME Transactions on Mechatronics, vol. 17, no. 6, pp. 1059-1067.

[9] Zhu Q, Xie X R, Li C, Xia G H and Liu Q, “Kinematic Self-Calibration Method for Dual-Manipulators Based on Optical Axis Constraint,” IEEE Access, vol. 7, pp. 7768-7782.

[10] Du G L, Liang Y H, Li C Q, P. X. Liu and D. Li, “Online Robot Kinematic Calibration Using Hybrid Filter with Multiple Sensors,” IEEE Transactions on Instrumentation and Measurement, vol. 69, no. 9, pp. 7092-7107.

[11] Zhang Y, Guo J W and Li X Y, “Study on Redundancy in Robot Kinematic Parameter Identification,” IEEE Access, vol. 10, pp. 60572-60584.

[12] I. Enebuse, M. Foo, B. S. K. K. Ibrahim, H. Ahmed, F. Supmak and O. S.Eyobu, “A Comparative Review of Hand-Eye Calibration Techniques for Vision Guided Robots,” IEEE Access, vol. 9, pp. 113143-113155.

[13] Sun J, Wang P, Qin Z K and Qiao H, “Effective self-calibration for camera parameters and hand-eye geometry based on two feature points motions,” IEEE/CAA Journal of Automatica Sinica, vol. 4, no. 2, pp. 370-380.

[14] R. Y. Tsai and R. K. Lenz, “Real time versatile robotics hand/eye calibration using 3D machine vision,” Proceedings 1988 IEEE International Conference on Robotics and Automation (ICRA), Philadelphia, PA, USA, pp. 554-561 vol.1.

[15] Jiang J F, Luo X, Xu S J, Luo Q S and Li M H, “Hand-Eye Calibration of EOD Robot by Solving the AXB = YCZD Problem,” IEEE Access, vol. 10, pp. 3415-3429.

[16] Zhong F X, Wang Z R, Chen W, He K J, Wang Y Q and Liu Y H, “Hand-Eye Calibration of Surgical Instrument for Robotic Surgery Using Interactive Manipulation,” IEEE Robotics and Automation Letters, vol. 5, no. 2, pp. 1540-1547.

[17] Jiang Z H, Zhou W G, Li H, Mo Y, Ni W C and Huang Q, “A New Kind of Accurate Calibration Method for Robotic Kinematic Parameters Based on the Extended Kalman and Particle Filter Algorithm,” IEEE Transactions on Industrial Electronics, vol. 65, no. 4, pp. 3337-3345.

[18] Zhang Y, Guo J W and Li X Y, “Study on Redundancy in Robot Kinematic Parameter Identification,” IEEE Access, vol. 10, pp. 60572-60584.

[19] Zhong X L, J.M. Lewis, and F.L.N. Nagy, “Autonomous robot calibration using a trigger probe,” Robotics and Autonomous Systems, vol.18, no.4, pp.395-410.

[20] M.A. Meggiolaro, S. Dubowsky, and C. Mavroidis, “Geometric and elastic error calibration of a high accuracy patient positioning system,” Mechanism and Machine Theory, vol.40, no.4, pp.415-427.

[21] Klimchik, B. Furet, S. Caro, and A. Pashkevich, “Identification of the manipulator stiffness model parameters in industrial environment,” Mechanism and Machine Theory, vol.90, pp.1-22.